HIRAGA, K. (1991). *Quasicrystals: the State of the Art*, edited by D. P. DIVICENZO & P. J. STEINHARDT, pp. 95-110. Singapore: World Scientific.
ISHIMASA, T., NISSEN, H.-U. & FUKANO, Y. (1984). Workshop on Physics of Small Particles, Gwatt, Switzerland, October 1984.
JARIĆ, M. V. (1990). *Period. Mineral.* **59**, 11-29.
KATZ, A. & DUNEAU, M. (1986). *J. Phys. (Paris)*, **47**, C3, 103-112.
KLITZING, R. (1992). Thesis, Univ. Tübingen, Germany.
KORTAN, A. R., BECKER, R. S., THIEL, F. A. & CHEN, H. S. (1990). *Phys. Rev. Lett.* **64**, 200-203.
KOWALEWSKI, G. (1938). *Der Keplersche Körper und andere mathematische Bauspiele*. Leipzig: Kohlers Antiq.
KRAMER, P. & NERI, R. (1984). *Acta Cryst.* A**40**, 580-587.
LEVINE, D. & STEINHARDT, P. J. (1984). *Phys. Rev. Lett.* **53**, 2477-2480.
LEVINE, D. & STEINHARDT, P. J. (1986). *Phys. Rev. B.* **34**, 596-616.
LEVITOV, L. S. (1988). *Commun. Math. Phys.* **119**, 627-666.
MACKAY, A. L. (1981*a*). *Kristallografiya*, **26**, 910-919.
MACKAY, A. L. (1981*b*). *Sov. Phys. Crystallogr.* **26**, 517-522.
NIIZEKI, K. & MITANI, H. (1987). *J. Phys. A: Gen. Phys.* **20**, L405-L410.
NISSEN, H.-U. (1990). *Quasicrystals, Networks, and Molecules of Fivefold Symmetry*, edited by I. HARGITTAI, ch. 11, pp. 181-199. New York: VCH.
NISSEN, H.-U. & BEELI, C. (1990). *Period. Mineral.* **59**, 31-67.
NISSEN, H.-U. & BEELI, C. (1993). *Int. J. Mod. Phys. B*, **7**, 1387-1413.
PAULING, L. (1985). *Nature (London)*, **317**, 512-514.
ROBINSON, R.M. (1975). *Comments on Penrose Tiles*. Berkeley: Univ. of California.
SASTRY, G. V. S., SURYANARAYANA, C., VAN SANDE, M. & VAN TENDELOO, G. (1978). *Mater. Res. Bull.* **13**, 1065.
SCHLEGEL, V. (1883). *Nova Acta Acad. Caesareae Leopold.-Carolin. Ger. Naturae Curiosorum*, **44**, 337-459. (Full journal: *Verhandlungen der Kaiserlichen Leopoldinisch-Carolinischen Deutschen Akademie der Naturforscher*, Halle, Germany.)
SHECHTMAN, D., BLECH, I., GRATIAS, D. & CAHN, J. W. (1984). *Phys. Rev. Lett.* **53**, 1951-1953.
SOCOLAR, J. E. S. (1989). *Phys. Rev. B*, **39**, 10519-10551.
SOCOLAR, J. E. S. & STEINHARDT, P. J. (1986). *Phys. Rev. B*, **34**, 617-647.
STAMPFLI, P. (1990). *Quasicrystals, Networks, and Molecules of Fivefold Symmetry*, edited by I. HARGITTAI, ch. 11, pp. 201-221. New York: VCH.
STEURER, W. & KUO, K. H. (1990). *Philos. Mag. Lett.* **62**, 175-182.
TANG, L.-H. (1990). *Period. Mineral.* **59**, 101-114.
WIDOM, M., STRANDBURG, K. J. & SWENDSEN, R. H. (1987). *Phys. Rev. Lett.* **58**, 706-709.

Acta Cryst. (1994). A**50**, 566–574

Convergent-Beam Electron Diffraction Study of Incommensurately Modulated Crystals. II. (3 + 1)-Dimensional Space Groups

BY MASAMI TERAUCHI, MARIKO TAKAHASHI* AND MICHIYOSHI TANAKA

Research Institute for Scientific Measurements, Tohoku University, Sendai 980, *Japan*

(*Received* 2 *July* 1993; *accepted* 20 *September* 1993)

Abstract

The convergent-beam electron diffraction (CBED) method for determining three-dimensional space groups is extended to the determination of the (3 + 1)-dimensional space groups for one-dimensional incommensurately modulated crystals. It is clarified than an approximate dynamical extinction line appears in the CBED discs of the reflections caused by an incommensurate modulation. The extinction enables the space-group determination of the (3 + 1)-dimensional crystals or the one-dimensional incommensurately modulated crystals. An example of the dynamical extinction line is shown using an incommensurately modulated crystal of $Sr_2Nb_2O_7$. Tables of the dynamical extinction lines appearing in CBED patterns are given for all the (3 + 1)-dimensional space groups of the incommensurately modulated crystal.

1. Introduction

The space groups of three-dimensional crystals can be determined by the convergent-beam electron diffraction (CBED) method. The method is based on dynamical extinction, which permits an unambiguous identification of 2_1 screw axes and glide planes. The dynamical extinction effect in electron diffraction at a symmetrical incidence was discussed theoretically by Cowley & Moodie (1959), Miyake, Takagi & Fujimoto (1960) and Cowley, Moodie, Miyake, Takagi & Fujimoto (1961). Goodman & Lehmpfuhl (1964) first observed the dynamical extinction as dark cross bands or lines in kine-

* Present address: NEC Corporation, Minamihashimoto 3-1-35, Sagamihara, Kanagawa 229, Japan.

matically forbidden reflection discs of CBED patterns of CdS. Gjønnes & Moodie (1965) developed a general theory of the dynamical extinction taking account of the interaction between not only zeroth-order Laue zone (ZOLZ) reflections but also higher-order Laue zone (HOLZ) reflections. Steeds, Rackham & Shannon (1978) reported a method of distinguishing between a 2_1 screw axis and a glide plane, which examines the characteristic appearance of the extinction line with the change of diffration condition. Another method to distinguish between those two symmetry elements was reported by Tanaka, Sekii & Nagasawa (1983), who investigated the symmetry of HOLZ lines with respect to the dynamical extinction line formed by the interaction of ZOLZ reflections. The dynamical extinction lines appearing in ZOLZ reflections of CBED patterns due to both ZOLZ and HOLZ interactions were tabulated for all the three-dimensional space groups by Tanaka *et al.* (1983) and later in a better form by Tanaka & Terauchi (1985). The dynamical extinction lines due to glide planes appearing in HOLZ reflections in CBED patterns were tabulated for all the three-dimensional space groups by Tanaka, Terauchi & Kaneyama (1988). As a result, it became clear that 181 of the 230 space groups can be uniquely identified using only the dynamical extinction lines. It is noted that the remaining 49 space groups can be identified by the examination of the intensity variation of the kinematically forbidden reflections with the change of diffraction condition. The space-group determination has been carried out successfully for many materials (for examples see Goodman & Whitfield, 1980; Steeds & Evans, 1980; Tanaka, Sekii & Ohi, 1985; Tanaka, 1987; Tanaka *et al.*, 1988).

Recently, attention has been paid to the determination of atom positions (structure analysis) by the CBED method (Vincent, Bird & Steeds, 1984; Tanaka & Tsuda, 1990, 1991) and to the determination of symmetries of higher-dimensional crystals or incommensurately modulated crystals and quasicrystals (Tanaka, Terauchi, Hiraga & Hirabayashi, 1985; Bendersky & Kaufman, 1986; Tanaka, Terauchi, Suzuki, Hiraga & Hirabayashi, 1987; Saito, Tanaka, Tsai, Inoue & Masumoto, 1992). Incommensurately modulated crystals do not have three-dimensional lattice periodicity and so are not expressed by three-dimensional space groups. The crystals, however, recover lattice periodicity in a space higher than three dimensions. de Wolff (1974, 1977) showed that a one-dimensional displacively and substitutionally modulated crystal can be described as a three-dimensional section of a $(3+1)$-dimensional periodic crystal. Janner & Janssen (1980) developed a more general approach to describe modulated crystals with n modulations as $(3+n)$-dimensional periodic crystals ($n=1, 2, \ldots$). Yamamoto (1982) derived a general structure-factor formula for the n-dimensionally modulated crystal ($n=1, 2, \ldots$), which holds for both displacively and substitutionally modulated crystals. Tables of all the $(3+1)$-dimensional space-group symbols for one-dimensional incommensurately modulated crystals of were given by de Wolff, Janssen & Janner (1981). Later, some corrections of the tables were reported by Yamamoto, Janssen, Janner & de Wolff (1985). The structure analysis of incommensurately modulated crystals using $(3+1)$-dimensional space groups has become familiar in the field of X-ray diffraction.

Fung, Steeds & Eades (1980) applied the CBED method to the study of incommensurately modulated transition-metal dichalcogenides. Steeds *et al.* (1985) applied the large-angle CBED method (Tanaka, Saito, Ueno & Harada, 1980) to the study of incommensurately modulated crystals of $NiGe_{1-x}P_x$. Tanaka *et al.* (1988) examined the symmetries of the incommensurate and fundamental reflections appearing in the CBED patterns obtained from the incommensurately modulated crystals of $Sr_2Nb_2O_7$ and Mo_8O_{23}. However, a $(3+1)$-dimensional analysis of the CBED patterns from incommensurately modulated crystals has not previously been given. The interrelation between the symmetries of CBED patterns and the $(3+1)$-dimensional point-group symbols for incommensurately modulated crystals was clarified theoretically and verified experimentally by Terauchi & Tanaka (1993). The CBED method is expected to be capable of extension to the determination of the $(3+1)$-dimensional space groups.

In the present study, we show theoretically in § 2 that dynamical extinction occurs for screw axes and glide planes of the $(3+1)$-dimensional crystal having an infinite dimension along the direction of the incommensurate modulation wave vector **k**. We also show in § 2 that approximate dynamical extinctions occur in the CBED patterns obtained from a finite specimen volume of the $(3+1)$-dimensional crystal. An example of dynamical extinction in a CBED pattern arising from a $(3+1)$-dimensional glide plane is given in § 3. Tables of the dynamical extinction lines are given for all $(3+1)$-dimensional space groups in § 4.

2. Dynamical extinction in CBED patterns

2.1. *Displacively modulated crystals*

The diffraction vector **G** for the $(3+1)$-dimensional crystals is written as

$$\mathbf{G}=h_1\mathbf{a}^*+h_2\mathbf{b}^*+h_3\mathbf{c}^*+h_4\mathbf{k},$$

where a set of $h_1h_2h_3h_4$ is a $(3+1)$-dimensional reflection index and $\mathbf{a}^*$, $\mathbf{b}^*$ and $\mathbf{c}^*$ are the reciprocal-lattice vectors of the base vectors **a**, **b** and **c** of the

average structure. The modulation wave vector $\mathbf{k}$ is written as

$$\mathbf{k}=k_1\mathbf{a}^*+k_2\mathbf{b}^*+k_3\mathbf{c}^*,$$

where one coefficient of k_i ($i=1$–3) is an irrational number and the others are rational. de Wolff (1974) showed that a one-dimensional incommensurately modulated crystal can be described as a three-dimensional section of a (3+1)-dimensional periodic crystal. In the (3+1)-dimensional description, an atom is not located at a point as in three-dimensional space but is expressed by a string, which extends along the fourth direction $\mathbf{a}_4$ perpendicular to the three-dimensional space R_3. The structure factor $F(h_1h_2h_3h_4)$ for the (3+1)-dimensional crystal is given by de Wolff (1974, 1977) as follows.

$$F(h_1h_2h_3h_4)=\sum_{\mu=1}^{N} f_\mu \exp 2\pi i(h_1\overline{x_1^\mu}+h_2\overline{x_2^\mu}+h_3\overline{x_3^\mu}) \times \int_0^1 \exp 2\pi i\Big\{\sum_{i=1}^{3}(h_i+h_4k_i)u_i^\mu(\overline{x_4^\mu}) + h_4\overline{x_4^\mu}\Big\}\,\mathrm{d}\overline{x_4^\mu}, \quad (1)$$

where

$$\overline{x_4^\mu}=(\overline{x_1^\mu}+n_1)k_1+(\overline{x_2^\mu}+n_2)k_2+(\overline{x_3^\mu}+n_3)k_3.$$

The symbols f_μ and $\overline{x_i^\mu}$ ($i=1$–3) are the atom form factor and the ith component of the atom position of the μth atom in the unit cell of the average structure, respectively. The symbol u_i^μ is the ith component of the displacement of the μth atom from the average atom position $\overline{x_i^\mu}$. $u_i^\mu(\overline{x_4^\mu})$ is a periodic function of the fourth coordinate $\overline{x_4^\mu}$. Since the atom in the (3+1)-dimensional space is continuous along the a_4 axis and discrete along R_3, the structure factor is expressed by the summation in R_3 and the integration along the a_4 axis.

The condition for dynamical extinction in CBED patterns can be found from the examination of the structure factors [(1)] for the two reflections, which are related by a glide plane or a screw axis of the (3+1)-dimensional space group concerned. For simplicity, we assume that the modulated structure belongs to the (3+1)-dimensional space group $P^{P2mm}_{1s\,1}$ and has the modulation wave vector $\mathbf{k}=k_3\mathbf{c}^*$. This space-group symbol implies: (i) the modulation wave vector $\mathbf{k}$ exists inside the first Brillouin zone of the average structure (P); (ii) the average structure belongs to the space group $P2mm$; (iii) the modulated structure has neither twofold rotation axes along the a axis nor mirror planes perpendicular to the c axis (subsymbol $\bar{1}$), these symmetries existing in the average structure; (iv) the modulated structure has glide planes (^m_s) perpendicular to the b axis with a shift of $\frac{1}{2}a_4$ along the a_4 axis (subsymbol s). The glide plane transforms an atomic row to another atomic row through the mirror plane perpendicular to the b axis and shifts the phase of the modulation wave by an amount π. For the glide plane (^m_s) of this (3+1)-dimensional space group, the structure factor $F(h_1h_2h_3h_4)$ [(1)] is written as

$$\begin{aligned}F(h_1h_2h_3h_4)=&\sum_{\mu=1}^{N} f_\mu \exp 2\pi i(h_1\overline{x_1^\mu}+h_2\overline{x_2^\mu}+h_3\overline{x_3^\mu}) \times \int_0^1 \exp 2\pi i[h_1u_1^\mu(\overline{x_4^\mu})+h_2u_2^\mu(\overline{x_4^\mu}) \\ &+(h_3+h_4k_3)u_3^\mu(\overline{x_4^\mu})+h_4\overline{x_4^\mu}]\,\mathrm{d}\overline{x_4^\mu} \\ &+\sum_{\mu=1}^{N} f_\mu \exp 2\pi i(h_1\overline{x_1^\mu}-h_2\overline{x_2^\mu}+h_3\overline{x_3^\mu}) \times \int_0^1 \exp 2\pi i[h_1u_1^\mu(\overline{x_4^\mu}+\tfrac{1}{2})-h_2u_2^\mu(\overline{x_4^\mu}+\tfrac{1}{2}) \\ &+(h_3+h_4k_3)u_3^\mu(\overline{x_4^\mu}+\tfrac{1}{2})+h_4\overline{x_4^\mu}]\,\mathrm{d}\overline{x_4^\mu},\end{aligned}$$

where

$$\overline{x_4^\mu}=(\overline{x_3^\mu}+n_3)k_3.$$

The shift of the integration range by half of the period about the a_4 axis yields the following equation.

$$\begin{aligned}F(h_1h_2h_3h_4)=&\sum_{\mu=1}^{N} f_\mu \exp 2\pi i(h_1\overline{x_1^\mu}+h_2\overline{x_2^\mu}+h_3\overline{x_3^\mu}) \times \int_0^1 \exp 2\pi i[h_1u_1^\mu(\overline{x_4^\mu})+h_2u_2^\mu(\overline{x_4^\mu}) \\ &+(h_3+h_4k_3)u_3^\mu(\overline{x_4^\mu})+h_4\overline{x_4^\mu}]\,\mathrm{d}\overline{x_4^\mu} \\ &+\exp(h_4\pi i)\sum_{\mu=1}^{N} f_\mu \exp 2\pi i(h_1\overline{x_1^\mu}-h_2\overline{x_2^\mu} \\ &+h_3\overline{x_3^\mu})\int_0^1 \exp 2\pi i[h_1u_1^\mu(\overline{x_4^\mu})-h_2u_2^\mu(\overline{x_4^\mu}) \\ &+(h_3+h_4k_3)u_3^\mu(\overline{x_4^\mu})+h_4\overline{x_4^\mu}]\,\mathrm{d}\overline{x_4^\mu}. \quad (2)\end{aligned}$$

Then, the following phase relations between the two structure factors are obtained for the (3+1)-dimensional glide plane (^m_s):

$$\begin{aligned}F(h_1h_2h_3h_4)&=F(h_1\bar{h}_2h_3h_4) \quad \text{for } h_4 \text{ even},\\ F(h_1h_2h_3h_4)&=-F(h_1\bar{h}_2h_3h_4) \quad \text{for } h_4 \text{ odd}.\end{aligned} \quad (3)$$

These relations are analogous to the phase relations between the two structure factors for the three-dimensional glide planes (Gjønnes & Moodie, 1965).

Figs. 1(*a*) and (*b*), respectively, illustrate a usual diffraction pattern and a CBED pattern expected from a crystal with the (3+1)-dimensional space group $P^{P2mm}_{1s\,1}$ at [100] incidence. The larger and smaller dots in Fig. 1(*a*) indicate the fundamental reflections ($h_4=0$) from the average structure and the incommensurate reflections ($h_4\neq 0$) originating from the modulation, respectively. The $00h_3h_4$ ($h_4=$ odd) reflections denoted by the crosses are kinematically

forbidden owing to the (3 + 1)-dimensional glide plane $\binom{m}{s}$ perpendicular to the b axis. For simplicity, only the first- and second-order incommensurate reflections are drawn. *Umweganregung* paths a and b in the ZOLZ to a kinematically forbidden reflection are shown with thick arrows. The two paths are geometrically equivalent with respect to the line (m–m) perpendicular to the b^* axis. Since every *Umweganregung* path to the kinematically forbidden reflection $00h_3h_4$ (h_4 = odd) contains an odd number of $F(0h_{2,i}h_{3,i}h_{4,i})$ with odd $h_{4,i}$, the following equation holds.

$$F(0h_{2,1}h_{3,1}h_{4,1})F(0h_{2,2}h_{3,2}h_{4,2})\ldots F(0h_{2,n}h_{3,n}h_{4,n}) \quad \text{for path } a$$
$$= -F(0\overline{h_{2,1}}h_{3,1}h_{4,1})F(0\overline{h_{2,2}}h_{3,2}h_{4,2})\ldots F(0\overline{h_{2,n}}h_{3,n}h_{4,n}) \quad \text{for path } b, \quad (4)$$

where

$$\sum_{i=1}^{n} h_{2,i} = 0, \quad \sum_{i=1}^{n} h_{3,i} = h_3, \quad \sum_{i=1}^{n} h_{4,i} = h_4 \ (h_4 = \text{odd}).$$

We omit the function of the excitation errors because they are the same for both paths a and b. The waves passing through the two paths are superposed on the $00h_3h_4$ (h_4 = odd) disc and cancel out because they have the same amplitude but different signs. When the projection of the Laue point parallel to the zone axis lies on the c^* axis, the excitation errors of the reflections for the two paths are kept the same. Then, a dynamical extinction line appears along the c^* axis (line A) in the kinematically forbidden discs of the CBED pattern, as shown in Fig. 1(b). In path c, the reflections are arranged in the reverse order to those in path b. When the $00h_3h_4$ (h_4 = odd) reflection is exactly excited, the two paths a and c are symmetric with respect to the bisector (m'–m') of the diffraction vector of the reflection and have the same excitation error. The waves passing through these paths have the same amplitude but different signs. That is,

$$F(0h_{2,1}h_{3,1}h_{4,1})F(0h_{2,2}h_{3,2}h_{4,2})\ldots F(0h_{2,n}h_{3,n}h_{4,n}) \quad \text{for path } a$$
$$= -F(0\overline{h_{2,n}}h_{3,n}h_{4,n})F(0\overline{h_{2,n-1}}h_{3,n-1}h_{4,n-1})\ldots$$
$$\times F(0\overline{h_{2,1}}h_{3,1}h_{4,1}) \quad \text{for path } c. \quad (5)$$

As a result, these two waves cancel out on the $00h_3h_4$ (h_4 = odd) disc, resulting in the dark line B perpendicular to line A. Line B is schematically drawn in the 0011 disc in Fig. 1(b). When a (3 + 1)-dimensional 2_1 screw axis $\binom{2}{s}$ exists parallel to the c axis, the same relations (4) and (5) hold for *Umweganregung* paths a, b and c as far as ZOLZ reflections are concerned. Then, the same dynamical extinction lines A and B are produced by the (3 + 1)-dimensional 2_1 screw axis. When lines A and B are formed by *Umweganregung* paths lying in the ZOLZ, these lines are written as A_2 and B_2, the subscript 2 indicating ZOLZ or two-dimensional interaction.

When *Umweganregung* takes routes in HOLZ (three-dimensional interaction), the (3 + 1)-dimensional glide plane produces only the dynamical

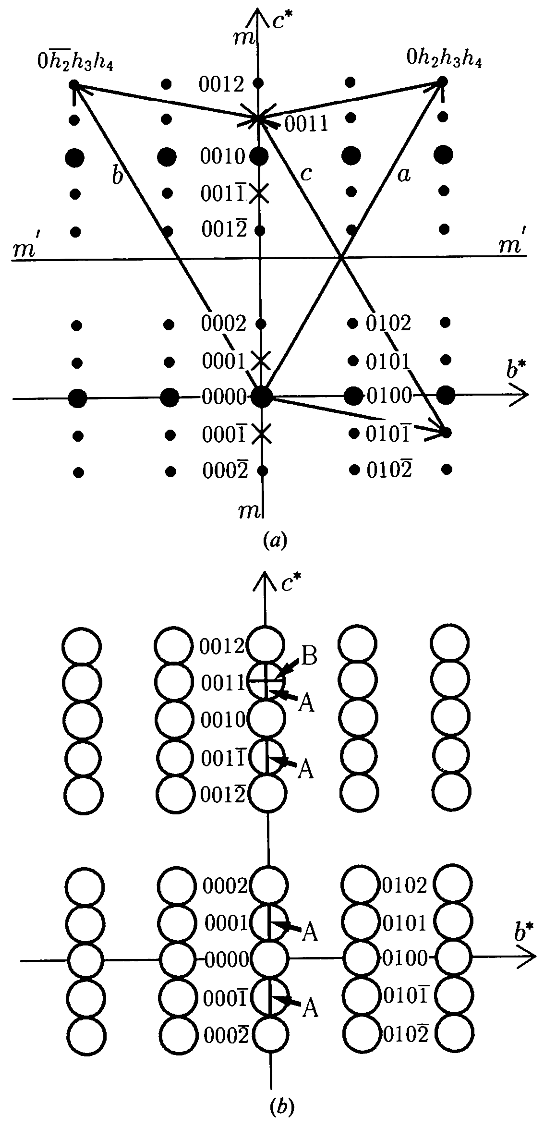

Fig. 1. (a) A schematic diffraction pattern expected from a crystal with the (3 + 1)-dimensional space group $P^{P2mm}_{\bar{1}s\bar{1}}$ at [100] incidence. The larger and smaller dots indicate the fundamental reflections ($h_4 = 0$) due to the average structure and the incommensurate ones ($h_4 \neq 0$) originating from the modulation, respectively. The $00h_3h_4$ (h_4 = odd) reflections denoted by crosses are kinematically forbidden owing to the (3 + 1)-dimensional glide plane $\binom{m}{s}$ perpendicular to the b axis. Thick arrows indicate *Umweganregung* paths to a kinematically forbidden reflection. (b) A corresponding schematic CBED pattern, where the kinematically forbidden reflection 0011 is assumed to be exactly excited. Dynamical extinction lines A are drawn in the forbidden reflections and line B in the exactly excited reflection.

extinction line A, but the $(3+1)$-dimensional 2_1 screw axis causes only line B. Then, it is possible to distinguish between the $(3+1)$-dimensional glide plane and the 2_1 screw axis through the three-dimensional interaction. These matters are attributed to the fact that different structure-factor relations hold for the glide plane (^m_s) perpendicular to the b axis and the 2_1 screw axis (^2_s) parallel to the c axis:

$$F(h_1h_2h_3h_4)=(-1)^{h_4}F(h_1\overline{h_2}h_3h_4) \quad \text{for the glide plane,} \tag{6}$$

$$F(h_1h_2h_3h_4)=(-1)^{h_4}F(\overline{h_1}\overline{h_2}h_3h_4) \quad \text{for the } 2_1 \text{ screw axis.} \tag{7}$$

For the dynamical extinction lines due to three-dimensional interaction, we use the symbols A_3 and B_3. Therefore, it has been clarified that the $(3+1)$-dimensional glide plane and 2_1 screw axis cause the dynamical extinction lines in the kinematically forbidden reflection discs of the CBED patterns. The results are exactly the same as in the cases of the three-dimensional glide plane and the 2_1 screw axis of usual three-dimensional crystals (Gjønnes & Moodie, 1965).

It should be noted that the above argument is correct when the diffraction pattern is obtained from an infinite specimen area, because the integration about $\overline{x_4^\mu}$ in (1) implies the summation of R_3 over an infinite number of the unit cells of the average structure along the direction of the modulation wave vector $\mathbf{k}$. The real CBED pattern, however, is obtained from a finite area of a crystal. Hence, it is necessary to use the structure factor, which takes account of the effect of the finite size, to discuss dynamical extinction lines in real CBED patterns. The structure factor for a finite specimen volume $F'(h_1h_2h_3h_4)$ has already been derived from (1) by rewriting the integration over a period along the a_4 axis with the summation over a finite number of three-dimensional sections of the atom strings (Terauchi & Tanaka, 1993). That is,

$$F'(h_1h_2h_3h_4)=\sum_{\mu=1}^{N} f_\mu \exp 2\pi i(h_1\overline{x_1^\mu}+h_2\overline{x_2^\mu}+h_3\overline{x_3^\mu}) \times \sum_{n_1}\sum_{n_2}\sum_{n_3}\exp 2\pi i\left\{\sum_{i=1}^{3}(h_i+h_4k_i)u_i^\mu+h_4\overline{x_4^\mu}\right\}, \tag{8}$$

where

$$\overline{x_4^\mu}=(\overline{x_1^\mu}+n_1)k_1+(\overline{x_2^\mu}+n_2)k_2+(\overline{x_3^\mu}+n_3)k_3,$$

$$N_1<n_1\le N_1', \quad N_2<n_2\le N_2', \quad N_3<n_3\le N_3'$$

and $N'=(N_1'-N_1)(N_2'-N_2)(N_3'-N_3)$ is the number of unit cells of the average structure in the specimen volume from which the CBED pattern is taken. The second line of (8) expresses the effect of the finite volume on the diffracted intensity. Then, the structure factor for the glide plane (^m_s) of the $(3+1)$-dimensional space group $P^{P2_1mm}_{1s1}$ that corresponds to (2) is written as

$$\begin{aligned}F'(h_1h_2h_3h_4) &= \sum_{\mu=1}^{N} f_\mu \exp 2\pi i(h_1\overline{x_1^\mu}+h_2\overline{x_2^\mu}+h_3\overline{x_3^\mu}) \\ &\times \sum_{n_3}\exp 2\pi i[h_1u_1^\mu+h_2u_2^\mu+(h_3+h_4k_3)u_3^\mu+h_4\overline{x_4^\mu}] \\ &+ \exp(h_4\pi i)\sum_{\mu=1}^{N} f_\mu \exp 2\pi i(h_1\overline{x_1^\mu}-h_2\overline{x_2^\mu}+h_3\overline{x_3^\mu}) \\ &\times \sum_{n_3}\exp 2\pi i[h_1u_1^{\mu'}-h_2u_2^{\mu'}+(h_3+h_4k_3)u_3^{\mu'}+h_4\overline{x_4^\mu}],\end{aligned} \tag{9}$$

where

$$\overline{x_4^\mu}=(\overline{x_3^\mu}+n_3)k_3, \quad u_i^{\mu'}=u_i^\mu.$$

For a given atom with a displacement u_i^μ (the first term), another with $u_i^{\mu'}$ (the second term) equal to u_i^μ cannot be found in the finite volume. That is, every atom in the finite volume cannot find a pairing atom related by the symmetry operation of a $(3+1)$-dimensional glide plane (^m_s) in the same volume because the pairing atom exists at a distance of infinity along the direction of the modulation. This implies that (8) cannot be transformed to (9) for the finite volume. This indicates that exact dynamical extinction does not occur in real CBED patterns. However, many atom pairs, which approximately satisfy $u_i^{\mu'}=u_i^\mu$, exist about half of the modulation wavelength apart.* Hence, (9) approximately holds when the specimen area has a dimension greater than the modulation wavelength along the direction of the modulation. Then, the same relation as (6) approximately holds for $F'(h_1h_2h_3h_4)$. Therefore, the approximate dynamical extinction line is produced when a specimen volume with a dimension larger than the wavelength along the direction of the modulation is illuminated.

For a $(3+1)$-dimensional 2_1 screw axis parallel to the c axis, it is already clear that the same relation as (7) approximately holds for $F'(h_1h_2h_3h_4)$. Then, the approximate dynamical extinction is also produced for the 2_1 screw axis. Therefore, the approximate dynamical extinction lines are expected to appear in

* Let us consider an atom whose displacement is expressed by a point on a modulation wave. Then, we consider the position with a phase difference of π on another modulation wave that is related to the original wave by the glide plane. If an atom is located at that position, exact dynamical extinction will take place. This cannot happen in the present instance, owing to the incommensurate nature of the modulation. However, we can find an atom very near that position with a phase difference nearly equal to π, causing approximate dynamical extinction.

real CBED patterns, owing to the (3+1)-dimensional glide plane and 2_1 screw axis of the displacively modulated crystals. It should be noted that an illuminated specimen volume with a dimension greater than the modulation wavelength is necessary for the (3+1)-dimensional space-group determination, whereas one unit cell of the average structure is enough to obtain the correct (3+1)-dimensional point-group symmetries (Terauchi & Tanaka, 1993). It is shown in § 3 that the CBED patterns from a displacively modulated crystal actually exhibit dynamical extinction.

2.2. *Substitutionally modulated crystals*

The substitutional modulation arises from a periodic variation of the site-occupation probability of atoms. This type of modulated structure is also described by a (3+1)-dimensional periodic structure. By substitution of zero for the displacements of atoms u_i^μ in (1), the structure factor for this type of modulated structures is written (de Wolff, 1974, 1977):

$$F(h_1h_2h_3h_4)=\sum_{\mu=1}^{N}\exp 2\pi i(h_1x_1^\mu+h_2x_2^\mu+h_3x_3^\mu)\times\int_0^1 f_\mu(x_4^\mu)\exp(2\pi ih_4x_4^\mu)\,\mathrm{d}x_4^\mu, \quad (10)$$

where

$$x_4^\mu=(x_1^\mu+n_1)k_1+(x_2^\mu+n_2)k_2+(x_3^\mu+n_3)k_3.$$

For simplicity, we again assume that the modulation wave vector is written as $\mathbf{k}=k_3\mathbf{c}^*$ and the modulated structure belongs to the (3+1)-dimensional space group $P^{P2mm}_{1s\,\bar{1}}$ as in the case of the displacively modulated structure. For the glide plane $\binom{m}{s}$ of this space group, the structure factor of (10) is written as

$$F(h_1h_2h_3h_4)=\sum_{\mu=1}^{N}\exp 2\pi i(h_1x_1^\mu+h_2x_2^\mu+h_3x_3^\mu)\times\int_0^1 f_\mu(x_4^\mu)\exp(2\pi ih_4x_4^\mu)\,\mathrm{d}x_4^\mu,$$
$$+\exp(h_4\pi i)\sum_{\mu=1}^{N}\exp 2\pi i(h_1x_1^\mu-h_2x_2^\mu+h_3x_3^\mu)\int_0^1 f_\mu(x_4^\mu)\exp(2\pi ih_4x_4^\mu)\,\mathrm{d}x_4^\mu, \quad (11)$$

where

$$x_4^\mu=(x_3^\mu+n_3)k_3.$$

Then, the following phase relation, which is the same as (3) and (6), is obtained for the two structure factors:

$$F(h_1h_2h_3h_4)=(-1)^{h_4}F(h_1\bar{h}_2h_3h_4).$$

When a (3+1)-dimensional 2_1 screw axis $\binom{2}{s}$ exists parallel to the c axis, the relation

$$F(h_1h_2h_3h_4)=(-1)^{h_4}F(\bar{h}_1\bar{h}_2h_3h_4)$$

holds between the two structure factors. Therefore, the dynamical extinction lines due to the (3+1)-dimensional glide plane and the 2_1 screw axis also appear for the substitutionally modulated crystals, when an infinite number of the unit cells of the average structure along the direction of the modulation wave vector $\mathbf{k}$ are illuminated.

The structure factor for the finite specimen volume $F'(h_1h_2h_3h_4)$ is needed to discuss dynamical extinction in real CBED patterns. It is written as

$$F'(h_1h_2h_3h_4)=\sum_{\mu=1}^{N}\exp 2\pi i(h_1x_1^\mu+h_2x_2^\mu+h_3x_3^\mu)\times\sum_{n_1}\sum_{n_2}\sum_{n_3}f_\mu(x_4^\mu)\exp(2\pi ih_4x_4^\mu), \quad (12)$$

where

$$N_1<n_1\le N_1',\quad N_2<n_2\le N_2',\quad N_3<n_3\le N_3'$$

and $N'=(N_1'-N_1)(N_2'-N_2)(N_3'-N_3)$ is the number of unit cells of the average structure included in the specimen volume (Terauchi & Tanaka, 1993). The second line of (12) expresses the effect of the finite volume. The structure factor corresponding to (11) is written as

$$F'(h_1h_2h_3h_4)=\sum_{\mu=1}^{N}\exp 2\pi i(h_1x_1^\mu+h_2x_2^\mu+h_3x_3^\mu)\times\sum_{n_3}f_\mu(x_4^\mu)\exp(2\pi ih_4x_4^\mu)$$
$$+\exp(h_4\pi i)\sum_{\mu=1}^{N}\exp 2\pi i(h_1x_1^\mu-h_2x_2^\mu+h_3x_3^\mu)\times\sum_{n_3}f_\mu'(x_4^\mu)\exp(2\pi ih_4x_4^\mu), \quad (13)$$

where

$$x_4^\mu=(x_3^\mu+n_3)k_3,\quad f_\mu'(x_4^\mu)=f_\mu(x_4^\mu).$$

In the substitutionally modulated case, the atom form factor f_μ is determined by the average over a large number of unit cells. A specimen volume about 10 nm in diameter and about 100 nm in thickness, from which CBED patterns are usually taken, is considered to be large enough to give the average value of the occupation or the average atom form factor. On the other hand, as discussed in § 2.1, a specimen volume with a dimension greater than the wavelength along the modulation is needed for the condition $f_\mu'(x_4^\mu)=f_\mu(x_4^\mu)$ in (13) to approximately hold. If this condition is satisfied, the same relation as (6) approximately holds again and, then, the approximate dynamical extinction line is produced. As a result of a similar argument, the same relation as (7) approximately holds for $F'(h_1h_2h_3h_4)$ for a (3+1)-dimensional 2_1 screw axis parallel to the c axis. Therefore, the dynamical extinction lines for the substitutionally modulated crystals are expected to

appear in real CBED patterns when they are taken from a finite volume with a dimension larger than the wavelength along the direction of the modulation and large enough to give the average value of the occupation or the average atom form factor.

3. Experimental results

Many materials of the $A_2B_2O_7$ family undergo phase transformations from the space group *Cmcm* to $Cmc2_1$ and further to $P2_1$ with decreasing temperature. For example, an incommensurate phase appears between the phase with $Cmc2_1$ and that with $P2_1$ in $La_2Ti_2O_7$ (Tanaka, Sekii & Ohi, 1985). $Sr_2Nb_2O_7$ transforms from the phase with $Cmc2_1$ into the incommensurate phase at 488 K with a modulation wave vector $\mathbf{k}=(\frac{1}{2}-\delta)\mathbf{a}^*$ ($\delta=0.009$–0.023) but does not transform into a phase with $P2_1$. The symmetry of the incommensurately modulated structure of $Sr_2Nb_2O_7$ is expressed by the (3+1)-dimensional space group $P^{C_s^c mc2_1}_{1s1}$ (Yamamoto, 1988).† The space-group symbol implies that the modulated structure has (3+1)-dimensional glide planes (^c_s) perpendicular to the *b* axis with a shift of $\frac{1}{2}\mathbf{c}+\frac{1}{2}\mathbf{a}_4$. Then, the reflections $h_10h_3h_4$ with $h_3+h_4=2n+1$ (n is an integer) are kinematically forbidden. Fig. 2(*a*) shows an electron diffraction pattern of the incommensurate phase of $Sr_2Nb_2O_7$ obtained with the [001] incidence at an accelerating voltage of 60 kV. The incommensurate reflections in which dynamical extinction lines appear are restricted to those with the indices $h_{1,\mathrm{even}}00h_{4,\mathrm{odd}}$ because $h_3=0$ at this incidence and $h_1+h_2=2n$, owing to the lattice type *C* of the average structure. The reflections in four columns indicated by arrows are incommensurate reflections due to the modulation. The reflections 0001, $000\bar{1}$, $200\bar{1}$ and $\bar{2}001$ indicated by thick arrows are kinematically forbidden but have intensities due to multiple diffraction. Other reflections are fundamental reflections due to the average structure. Fig. 2(*b*) shows a CBED pattern corresponding to Fig. 2(*a*), taken from a 3 nm-diameter specimen area. It is noted that the excitation errors for two *Umweganregung* paths to a kinematically forbidden reflection, which are geometrically equivalent about the a^* axis, are the same at this incidence. The kinematically forbidden reflections indicated by arrows show no intensity. This is a result of dynamical extinction in the (3+1)-dimensional crystal. Dynamical extinction does not appear as a line drawn in Fig. 1(*b*) because the size of the diffraction disc is set small to avoid the overlapping of the diffraction discs and the width of the dynamical extinction line exceeds the disc size. Fig. 2(*c*) shows a CBED pattern taken at a slightly tilted incidence towards the b^* axis from that for Fig. 2(*b*) or the [001] incidence. At this incidence, the excitation errors, which were equivalent for the pairs of *Umweganregung* paths in Fig. 2(*b*), are no longer the same. Then, it is seen that the kinematically forbidden reflections indicated by thick arrows have intensities, owing to an incomplete cancellation of the waves coming through the paths. This result also proves that the disappearance of intensity in Fig. 2(*b*) is caused by dynamical extinction. It is noted that an illuminated specimen area of 3 nm diameter is larger than the modulation wavelength of 0.786 nm. It has been revealed experimentally that dynamical extinction occurs from the (3+1)-dimensional glide plane for a displacively modulated crystal. These results confirm the theoretical result derived in § 2. Thus, the dynamical extinction enables the determination of the space groups of the (3+1)-dimensional crystals or the one-dimensional incommensurately modulated crystals. Tabulation of the dynamical extinction lines expected for all the (3+1)-dimensional space groups is of great importance for the space-group determination.

4. Tables of dynamical extinction lines

Dynamical extinction lines, which are expected to appear in the kinematically forbidden incommensurate-reflection discs of the CBED patterns, are tabulated for all the (3+1)-dimensional space groups. The labels and symbols of the (3+1)-dimensional space groups used here are the same as those given by de Wolff *et al.* (1981), the direction of the incommensurate component of the modulation wave vector being taken along the *c* axis. In the following tables, the reflection indices *hklm* are used instead of the $h_1h_2h_3h_4$ used in the previous sections.

For example, the table of dynamical extinction lines for the (3+1)-dimensional space groups $P^{A2aa}_{1s\bar{1}}$ is shown in Table 1. The label 37*b*.15.2 is the (3+1)-dimensional-space-group number. The label consists of three numbers: (1) 37 is the number of the three-dimensional space group *A*2*aa* for the average structure given in *International Tables for Crystallography* (1989) together with a letter *b* indicating a crystal setting; (2) 15 is the number of a (3+1)-dimensional Bravais class; (3) 2 distinguishes the symmetry of the modulation wave, indicating $\bar{1}\,s\,\bar{1}$ in this case. The incident-beam direction is denoted [*uvw*] referred to the lattice of the average structure. The reflections *h*0*lm* with $h+m=2n+1$ (n is an integer) are kinematically forbidden owing to the (3+1)-dimensional glide plane $s+a_1$ perpendicular to the *b* axis with a shift of $\frac{1}{2}\mathbf{a}+\frac{1}{2}\mathbf{a}_4$. The subscript of a_1 denotes the first

† In the tables of de Wolff *et al.* (1981), the direction of the incommensurate component of the modulation wave vector is taken along the *c* axis. There, the space group $P^{C_s^c mc2_1}_{1s1}$ is written as $P^{A^a_s 2_1 am}_{1s1}$. In the present case, the direction of the modulation is taken along the *a* axis because of the use of the space-group symbol widely accepted for the average structure.

glide plane between two a glide planes of the space group $A2aa$. Table 1 implies the following items: (1) At the [100] incidence, dynamical extinction lines A_2 and A_3 appear in the kinematically forbidden reflection discs with the indices $00l_em_o$ owing to the glide plane $s+a_1$. The subscripts of l_e and m_o, respectively, indicate an even number of l and an odd number of m. The incommensurate reflections in which dynamical extinction lines appear are restricted to those with the indices $00l_em_o$ because $h=0$ at this incidence and $k+l=2n$ owing to the lattice type A of the average structure. When a kinematically forbidden reflection $00l_em_o$ is exactly excited at the [100] incidence, dynamical extinction line B_2 appears in the reflection disc. (2) At the [010], $[uv0]$ and $[0vw]$ incidences, no dynamical extinction lines appear. (3) At the $[u0w]$ incidence, lines A_2 and A_3 appear in the discs $h0l_em$ under the restriction of $h+m=2n+1$ (n is an integer), owing to the glide plane $s+a_1$. When the reflection $h0l_em$ is exactly excited, line B_2 appears in the disc.

Table 1. *Dynamical extinction lines expected at two incident directions for the* (3+1)*-dimensional space group* P^{A2aa}_{1s1}

l_e = even, m_o = odd.

Space group	Incident-beam direction [100]		[010]	[uv0]	[0vw]	[u0w]	
37*b*.15.2 P^{A2aa}_{1s1}	$00l_em_o$ $s+a_1$	A_2 B_2 A_3				$h0l_em$ $h+m$ $=2n+1$ $s+a_1$	A_2 B_2 A_3

The table for the triclinic lattice of the average structure is omitted because dynamical extinction does not occur. Table 2 shows the expected dynamical extinction lines for the monoclinic lattice of the average structure and Tables 3, 4, 5 and 6 those for the orthorhombic, tetragonal, trigonal and hexagonal lattices, respectively.*

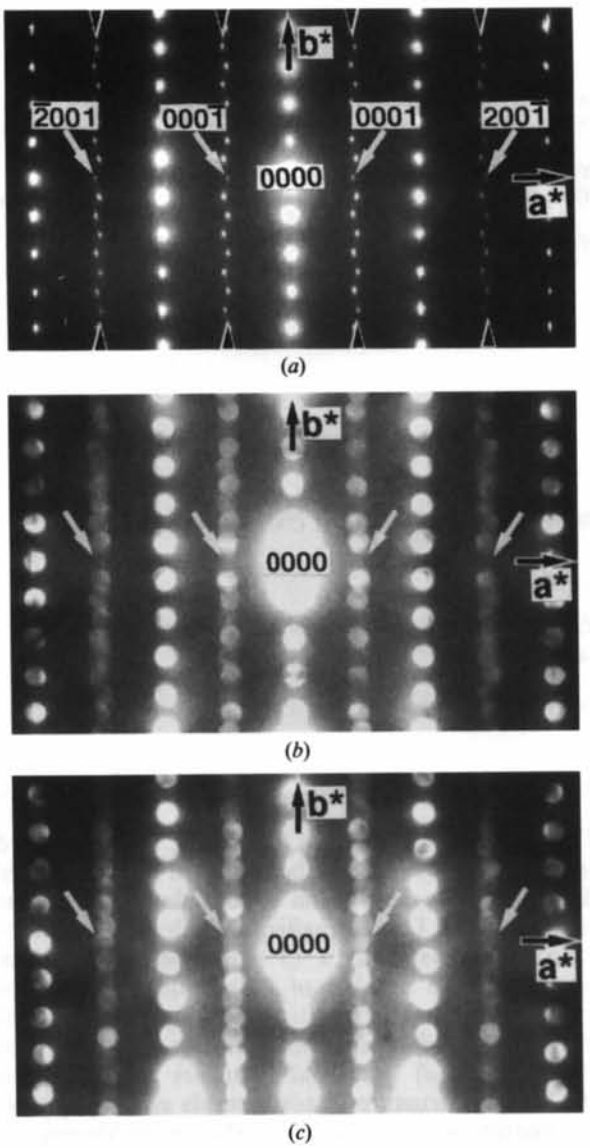

Fig. 2. (*a*) An electron diffraction pattern of the incommensurate phase of $Sr_2Nb_2O_7$ obtained with [001] incidence at an accelerating voltage of 60 kV. (*b*) A corresponding CBED pattern. The kinematically forbidden reflections indicated by arrows show no intensity (dynamical extinction). (*c*) A CBED pattern taken with an incidence slightly tilted towards the b^* direction. The forbidden reflections have intensities because of an incomplete cancellation of the waves.

The authors are grateful to Dr A. Yamamoto of the National Institute for Research in Inorganic Materials for useful discussions. The present work was partly supported by a Grant in Aid of Scientific Research from the Ministry of Education, Science and Culture, Japan.

* Tables 2, 3, 4, 5 and 6 have been deposited with the British Library Document Supply Centre as Supplementary Publication No. SUP 71810 (65 pp.). Copies may be obtained through The Managing Editor, International Union of Crystallography, 5 Abbey Square, Chester CH1 2HU, England.

References

BENDERSKY, L. A. & KAUFMAN, M. J. (1986). *Philos. Mag.* **B53**, L75–L80.

COWLEY, J. M. & MOODIE, A. F. (1959). *Acta Cryst.* **12**, 360–367.

COWLEY, J. M., MOODIE, A. F., MIYAKE, S., TAKAGI, S. & FUJIMOTO, F. (1961). *Acta Cryst.* **14**, 87–88.

FUNG, K. K., STEEDS, J. W. & EADES, J. A. (1980). *Physica (Utrecht)*, **B99**, 47–50.

GJØNNES, J. & MOODIE, A. F. (1965). *Acta Cryst.* **19**, 65–67.

GOODMAN, P. & LEHMPFUHL, G. (1964). *Z. Naturforsch. Teil A*, **19**, 818–820.

GOODMAN, P. & WHITFIELD, H. J. (1980). *Acta Cryst.* **A36**, 219–228.

International Tables for Crystallography (1989). Vol. A Dordrecht: Kluwer Academic Publishers.

JANNER, A. & JANSSEN, T. (1980). *Acta Cryst.* A**36**, 399–408, 408–415.
MIYAKE, S., TAKAGI, S. & FUJIMOTO, F. (1960). *Acta Cryst.* **13**, 360–361.
SAITO, M., TANAKA, M., TSAI, A. P., INOUE, A. & MASUMOTO, T. (1992). *Jpn. J. Appl. Phys.* **31**, L109–L112.
STEEDS, J. W., BIRD, D. M., EAGLESHAM, D. J., MCKERNAN, S., VINCENT, R. & WITHERS, R. L. (1985). *Ultramicroscopy*, **18**, 97–110.
STEEDS, J. W. & EVANS, N. S. (1980). Proceedings of the 38th Annual Meeting of the Electron Microscopy Society of America, pp. 188–191.
STEEDS, J. W., RACKHAM, G. M. & SHANNON, M. D. (1978). *Inst. Phys. Conf. Ser.* No. 41, pp. 135–139.
TANAKA, M. (1987). Proceedings of the 45th Annual Meeting of the Electron Microscopy Society of America, pp. 20–23.
TANAKA, M., SAITO, R., UENO, K. & HARADA, Y. (1980). *J. Electron Microsc.* **29**, 408–412.
TANAKA, M., SEKII, H. & NAGASAWA, T. (1983). *Acta Cryst.* A**39**, 825–837.
TANAKA, M., SEKII, H. & OHI, K. (1985). *Jpn. J. Appl. Phys.* **24**, Supplement, pp. 814–816.
TANAKA, M. & TERAUCHI, M. (1985). *Convergent-Beam Electron Diffraction*. Tokyo: JEOL-Maruzen.
TANAKA, M., TERAUCHI, M., HIRAGA, K. & HIRABAYASHI, M. (1985). *Ultramicroscopy*, **17**, 279–286.
TANAKA, M., TERAUCHI, M. & KANEYAMA, T. (1988). *Convergent-Beam Electron Diffraction* II. Tokyo: JEOL-Maruzen.
TANAKA, M., TERAUCHI, M., SUZUKI, S., HIRAGA, K. & HIRABAYASHI, M. (1987). *Acta Cryst.* B**43**, 494–501.
TANAKA, M. & TSUDA, K. (1990). Proceedings of the XIIth International Congress for Electron Microscopy, Seattle, USA, pp. 518–519.
TANAKA, M. & TSUDA, K. (1991). Proceedings of the 26th Meeting of the Microbeam Analysis Society, San Jose, USA, pp. 145–146.
TERAUCHI, M. & TANAKA, M. (1993). *Acta Cryst.* A**49**, 722–729.
VINCENT, R., BIRD, D. M. & STEEDS, J. W. (1984). *Philos. Mag. A*, **50**, 745–763, 765–786.
WOLFF, P. M. DE (1974). *Acta Cryst.* A**30**, 777–785.
WOLFF, P. M. DE (1977). *Acta Cryst.* A**33**, 493–497.
WOLFF, P. M. DE, JANSSEN, T. & JANNER, A. (1981). *Acta Cryst.* A**37**, 625–636.
YAMAMOTO, A. (1982). *Acta Cryst.* A**38**, 87–92.
YAMAMOTO, A., JANSSEN, T., JANNER, A. & DE WOLFF, P. M. (1985). *Acta Cryst.* A**41**, 528–530.
YAMAMOTO, N. (1988). *Solid State Phys.* **23**, 547–556.

Acta Cryst. (1994). A**50**, 574–579

On the Structure Factor for Commensurate Modulated Structures

BY F. PARISI

Departamento de Física, Comisión Nacional de Energía Atómica, Avda del Libertador 8250, (1429) *Buenos Aires, Argentina*

(*Received* 10 *September* 1993; *accepted* 4 *January* 1994)

Abstract

A superstructure may be looked upon as a commensurate modulated structure and be described through the superspace formalism. It can be studied using low- or high-symmetry superspace groups. The possibility of adopting a high-symmetry description is related to the existence of at least two independent three-dimensional sections in the supercrystal with the same space-group symmetry. The usual structure-factor formula for commensurate structures [Yamamoto (1982). *Acta Cryst.* A**38**, 87–92] includes just one of these sections, thus allowing for a low-symmetry description only. A very simple generalization of this in the superspace formalism is presented, which allows for the use of either low- or high-symmetry superspace groups in the structural analysis. The reasons for a seemingly successful refinement found in the literature, making use of the high-symmetry description, are discussed.

1. Introduction

The superspace formalism (de Wolff, 1974; Janner & Janssen, 1977, 1980) has been shown to be a powerful tool for the description of modulated incommensurate phases. This formalism includes the definition of a supercrystal in a $(3 + d)$-dimensional space, where d is the number of independent modulation wave vectors. The multidimensional construction includes $(3 + d)$-dimensional atomic positions and $(3 + d) \times (3 + d)$ thermal tensors (Yamamoto, 1982*a*). The structure-factor formula and the symmetry operators are referred to this multidimensional space. The symmetry groups of this space are often called superspace groups (SSGs).

The superspace formalism has also been employed in the structural analysis of commensurate phases by Yamamoto & Nakazawa (1982), Yamamoto (1983), Hogervorst & Helmholdt (1988) and Sciau & Grebille (1989), among others. Their principle